Proc. Natl. Acad. Sci. USA
Vol. 88, pp. 3623–3627, May 1991
Cell Biology

The first milliseconds of the pore formed by a fusogenic viral envelope protein during membrane fusion

(influenza hemagglutinin/fibroblast/membrane capacitance/patch clamp/fusion pore)

A. E. SPRUCE*, A. IWATA, AND W. ALMERS

Department of Physiology and Biophysics, University of Washington, Seattle, WA 98195

Communicated by Bertil Hille, January 29, 1991 (received for review December 12, 1990)

ABSTRACT **Fibroblasts expressing the influenza virus hemagglutinin on their plasma membrane were patch clamped while they fused to erythrocytes. An increase in the fibroblast's membrane capacitance indicated the opening of the "fusion pore," the first aqueous connection between the fusing cells. We show here that the capacitance increase is preceded by a brief current transient, generated as the erythrocyte discharges its membrane potential through the nascent fusion pore. This signal allows one to calculate the pore conductance during the first milliseconds of its existence. The pore conductance jumps from 0 to ≈150 pS and then grows more gradually over the subsequent tens of milliseconds until growth is arrested. The initial conductance is similar to that of a large ion channel and suggests that the pore is initially only 1–2 nm wide. Hence, we are probably observing events caused by only a small number of hemagglutinin molecules.**

Membrane fusion, a fundamental event in cell biology, is probably mediated by a wide variety of fusogenic proteins. The only such proteins identified so far are the "spike" proteins of enveloped viruses. Among them, the hemagglutinin (HA) of the influenza virus is the best characterized (1–3), but the mechanism of HA-mediated fusion remains unclear.

In fibroblasts expressing HA on their cell surface (4), single fusion events can be studied in real time. These fibroblasts bind erythrocytes (RBCs) and fuse with them when HA is activated by acidification. Fusion begins with the formation of an aqueous connection between the two cells. This "fusion pore," estimated to be no more than 9 nm (5) or 4 nm (6) wide initially, later dilates to at least 100 nm (4) and beyond. In previous work (6), we have monitored the conductance of the pore by analyzing the passage of sinusoidally alternating current between fibroblast and RBC. The pore conductance appeared to jump quickly to ≈600 pS and increased slowly thereafter, as if the pore opened suddenly and then continued to dilate over minutes. These measurements could resolve events lasting longer than 10 ms.

Fusion pores also form during exocytosis when secretory vesicles fuse with the plasma membrane of a secreting cell. In exocytic fusion, the initial pore conductance doubles within only 1–2 ms at 22°C (7). To see whether similarly rapid events also occur in HA-mediated fusion, we now apply a method that captures early fusion events at millisecond resolution (7, 8). We find that the initial conductance of the fusion pore is only 150 pS, smaller than previously thought.

METHODS

The methods for culturing fibroblasts expressing HA in their plasma membrane (NIH 3T3HA-b2; see ref. 9), for activating the HA by trypsin treatment, and for decorating the trypsin-treated fibroblasts with fresh human RBCs have all been described (6). Experiments were done at 24°C–30°C [mean, 28.1 ± 0.2°C (SEM); $n = 49$] in either NaCl buffer (140 mM NaCl/2.5 mM KCl/5 mM $MgCl_2$/2 mM $CaCl_2$/2 mM Na Hepes, pH 7.4) or, more frequently, in an "impermeant buffer" (155 mM *N*-methylglucamine gluconate or *N*-methylglucamine aspartate/5 mM $MgCl_2$/2 mM Cs Hepes buffer, pH 7.4), which suppressed the reversible, acid-induced conductance increase observed before (6). Electrical recordings from fibroblasts were made in the "whole-cell" mode (10) using micropipettes containing 155 mM Cs glutamate, 5 mM $MgCl_2$, 5 mM bis(2-aminophenoxy)ethane-*N*,*N*,*N*′,*N*′-tetraacetate (BAPTA), and 10 mM K Hepes (pH 7.4). In experiments in NaCl buffer, K^+ replaced Cs^+. Small, solitary fibroblasts (capacitance, 10–24 pF) decorated with a single RBC were voltage clamped at holding potentials of −78 to +14 mV. The electrical admittance between the inside and outside of the fibroblast was measured by superimposing a voltage sinusoid (30 mV peak to peak; frequency, 320 Hz) on the holding potential. The resulting sinusoidal current was separated by a lock-in amplifier (11) into imaginary (capacitance, 90° out of phase) and real components (G_{ac}, in phase with the voltage). In most experiments, capacitance and G_{ac} were measured only intermittently (7, 8) by applying the sinusoid in 31.2-ms-long bursts. This allowed us to record small currents related to fusion in the 281.3-ms intervals between bursts. Current, G_{ac}, and capacitance were stored on FM tape (Racal store 4 DS) and played into a digital computer. Current was low-pass filtered (5 kHz, four-pole Bessel), digitized at 11 kHz, and then further low-pass filtered digitally (12) to a corner frequency of 2 kHz. In some experiments, the voltage sinusoid was applied continuously, and C and G_{ac} were digitized at 320 Hz. Unless indicated otherwise, means ± SE are given.

Conductivity of Pipette Solution. We measured the resistance of pipettes filled with, and immersed in, either 0.1 M NaCl or the Cs glutamate solution. Since micropipette pullers pull pairs of pipettes with the same tip size, the conductivities of the two solutions can be compared by measuring the conductance of micropipette pairs. The resistance in Cs glutamate was 0.78 ± 0.05 ($n = 9$) times that in 0.1 M NaCl. Following Robinson and Stokes (13), the conductivity of 0.1 M NaCl is 10.7 mS/cm at 25°C and, with a temperature coefficient of 1.26, it is 12.01 mS/cm at 30°C. Hence, our Cs glutamate solution at 30°C has a conductivity of 12.01/0.78 = 15.4 mS/cm, and a resistivity of 65 Ω·cm.

RESULTS

Time-Resolved Admittance Measurements. After a RBC has fused with a fibroblast, the surface area of the cell pair is

The publication costs of this article were defrayed in part by page charge payment. This article must therefore be hereby marked "*advertisement*" in accordance with 18 U.S.C. §1734 solely to indicate this fact.

Abbreviations: RBC, erythrocyte; HA, influenza virus hemagglutinin.

*Present address: Department of Zoology, University of Washington, Seattle, WA 98195.

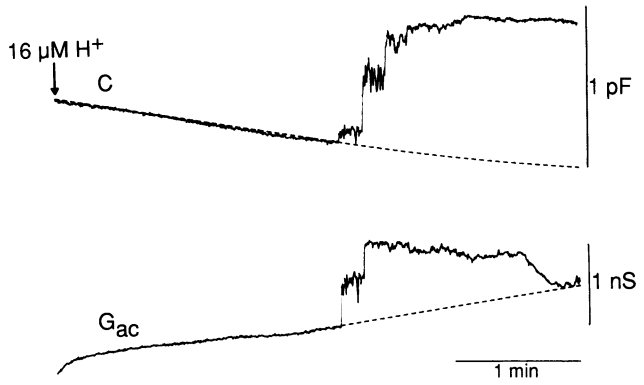

FIG. 1. Capacitance (C) and G_{ac} changes in a fibroblast during fusion with an RBC. Trace starts 1.5 min after the recording pipette and the cytosol became connected. H^+ was applied in a stream of solution similar to external buffer except that 20 mM *N*-methylglucamine succinate replaced 2 mM Na Hepes. This acidic solution (pH 4.8) flowed from the 5-μm-diameter tip of a perfusion micropipette placed within 100 μm of the cell pair. The dashed baseline for the C trace continues a slow decline in capacitance that is unrelated to fusion and probably due to endocytosis; it was generated as described (6). The G_{ac} baseline extrapolates the section of the trace immediately before fusion. Impermeant buffer; the fibroblast was held at −48 mV, and its initial capacitance was 21 pF.

larger than that of the fibroblast alone. Since all biological membranes have an electrical capacitance of 10 fF/μm², this change in surface area may be assayed by measuring the plasma membrane capacitance. Fig. 1 plots the capacitance (C) and conductance (G_{ac}) of a fibroblast with a single attached RBC. As described (6), the conductance is measured with alternating current in order to include conductive pathways in series with an electrical capacitance—i.e., intercellular junctions with the RBC. Two minutes after HA was activated by external acidification, the capacitance increased in unequal steps, while G_{ac} increased and then declined. The final value of the capacitance change (0.93 pF in Fig. 1; mean, 0.90 ± 0.03 pF; range, 0.64–1.09 pF; n = 17) represents the added 90-μm² area of a single human RBC (0.91 pF in ref. 6). Both the gradual increase in capacitance and the transient increase in G_{ac} result from a HA-mediated aqueous connection between the cytosols of fibroblast and RBC (6). The full value of the RBC capacitance is revealed only gradually because the connection is initially narrow, preventing complete invasion of the RBC by the sinusoid. Indeed, the increase of the capacitance to its final value can be used to calculate how the conductance of the connection increases with time, and the transient increase in G_{ac} can be similarly used. We now explore the beginning of fusion in four successive analyses (Figs. 2–5) whose temporal resolution progresses from seconds to milliseconds.

Fig. 2 analyzes early portions of the fusion event in Fig. 1. The capacitance and G_{ac} traces were each used to calculate the conductance of the developing cell–cell junction (6, 7). The conductance increased quickly to ≈0.6 nS (leftmost arrowhead), reflecting the opening of a fusion pore. It remained stable for >10 s until a second step occurred, followed 12 s later by a third step. The conductance continued to grow, but further steps, if present, were obscured by increasing noise. It is unknown whether the second and third steps arose from additional fusion pores opening between the RBC and fibroblast or from a stepwise dilation of the first pore. If conductances are converted into approximate pore diameters (see Fig. 3 legend), the levels indicated by the arrowheads indicate either three pores of diameters 2.9, 4.6, and 4.4 nm, or a single pore whose diameter increases from 2.9 to 5.6 and then to 7.4 nm.

When viewed on the time scale of Fig. 2*B*, the first increase in conductance appeared as a step in 44 of 65 similar recordings. The conductance then fluctuated around 500–700 pS (625 ± 67 pS; n = 44) for tens of seconds (median, 15 s; range, 4 s to >120 s) as in Fig. 2*B*. In 16 of the 44 recordings, one or two subsequent steps could be discerned. In the remaining recordings, the subsequent conductance increase did not contain obvious steps (e.g., see figure 2 in ref. 6). Either the conductance increased gradually, or it fluctuated so rapidly between different levels that steps were obscured.

Fig. 3*A* shows the beginning of a fusion at the highest temporal resolution we have achieved with time-resolved admittance measurements. A sinusoidal voltage was applied continuously and the capacitance and G_{ac} were measured every 3.1 ms. The pore conductance (Fig. 3*B*) is calculated from each of the two traces in Fig. 3*A*. It increased, declined again for a short period, and then fluctuated between 100 and 800 pS for the remaining period. Fig. 3*C* shows an average of five fusions analyzed as in Fig. 3*B*. The first few points during the conductance change are unreliable as they are probably contaminated by a current transient like that in Fig. 4 (see legend of Fig. 3). If one ignores them, Fig. 3*C* suggests that

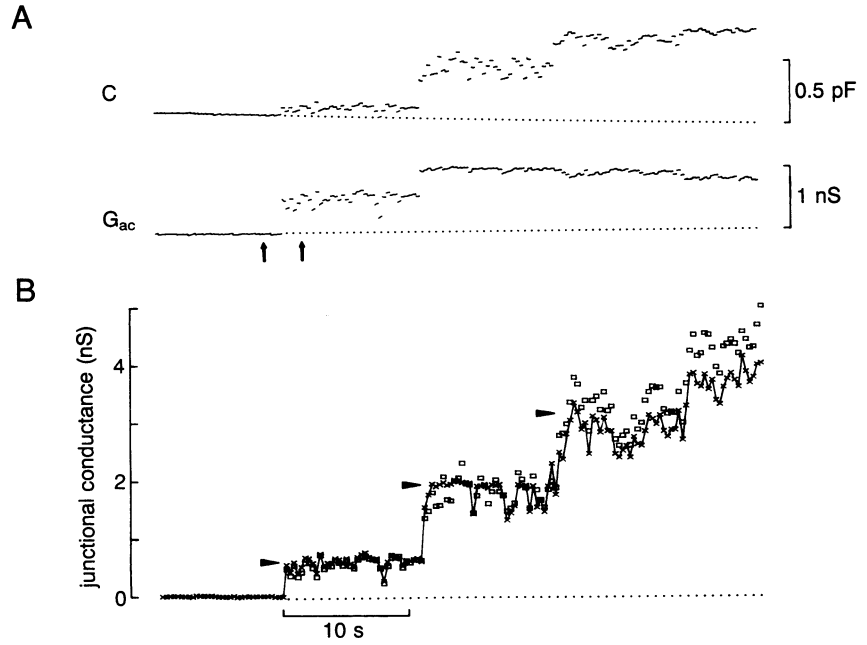

FIG. 2. (*A*) Traces in Fig. 1 replotted on a faster time scale; arrows mark the section explored in Fig. 4. (*B*) Junctional conductance (g) calculated from traces in *A* after subtracting baselines (7, 8). Values of g represented by squares were calculated from the C trace by $g = (2\pi f C_{RBC})/\{[C_{RBC}/(C-1)]^{1/2}\}$, where f is the frequency of the sinusoid (320 Hz) and C_{RBC} is the amplitude of the final capacitance deflection (927 fF). Values of g represented by crosses were calculated from G_{ac} by $g = (2G_{ac})/\{1 + n[1 - (G_{ac}/\pi f C_{RBC})^2]^{1/2}\}$, where n = 1 while $C < C_{RBC}/2$, and −1 otherwise. The arrowheads (at 0.62, 1.97, and 3.25 nS) estimate the three conductance levels of the fibroblast–RBC junction.

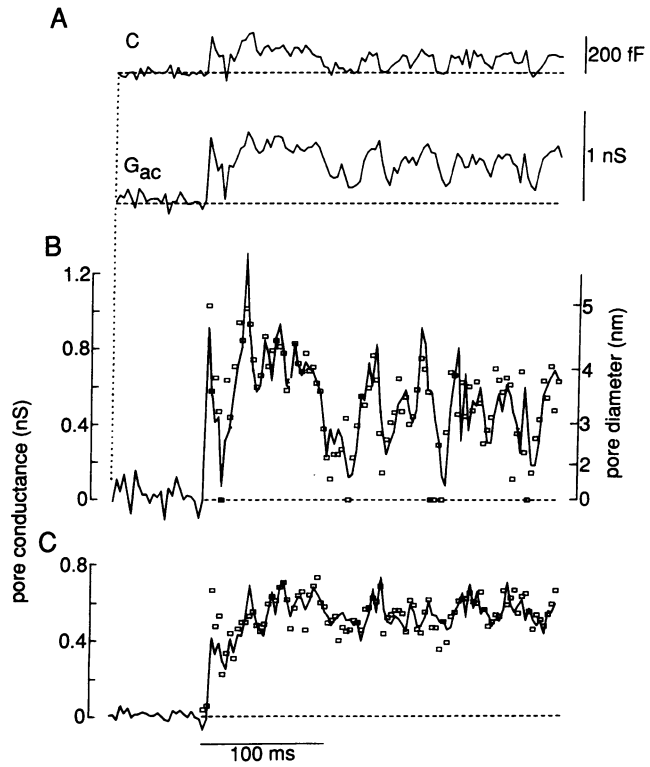

FIG. 3. (*A*) Fast capacitance and G_{ac} recordings at the beginning of a fusion. Voltage sinusoid applied continuously. (*B*) Pore conductance calculated from the capacitance (boxes) and G_{ac} traces in *A* (solid line). The right-hand ordinate converts conductance into the approximate pore diameter (see *Discussion*), assuming a pore length of 15 nm. (*C*) Average pore conductances from five fusions. The first four measurements after the capacitance and G_{ac} changes are unreliable because they are probably contaminated by current transients as in Fig. 4. Assuming the initial pore conductance g_i = 150 pS (see Table 1) and C_{RBC} = 0.91 pF, spikes are expected to decline with a time constant of 5.6 ms if the pore conductance remains constant. With a mean peak amplitude of 20 pA, current during a spike would be 7 pA after one time constant and 3 pA after another. A current of 3 pA would correspond to 100 pS since G_{ac} is measured with a 30-mV sinusoid. A 100-pS contamination extending over two time constants (11.2 ms) is clearly significant; hence, the first four points of the conductance jumps should be ignored in *B* and *C*.

the final conductance of 500–600 pS is not reached instantly. Hence, the 500- to 600-pS fusion pore has smaller, short-lived precursors that are not well resolved.

The large conductance fluctuations in Fig. 3*B* appeared in all but one of four other similar experiments. In Fig. 2*B*, such fluctuations were less obvious because capacitance and G_{ac} measurements were made only once every 300 ms and represent averages over 31-ms intervals. If the conductance in Fig. 3*B* is due to a single pore, the traces suggest that the pore diameter varied between <1.6 nm and >3.9 nm (right-hand ordinates).

A Current Transient Marks the Opening of the Fusion Pore. To explore the earliest fusion events in greater detail, a small section of Fig. 2*A* (arrows) is replotted vertically in Fig. 4 (*Right*) on an expanded abscissa. Because capacitance and G_{ac} were measured only intermittently, the traces show discrete points connected by lines. Each of the traces on the left shows the current collected from the cell during the period preceding the capacitance and G_{ac} measurements on the right. Halfway up the vertical traces, small increases in capacitance and G_{ac} mark the beginning of fusion. The current trace immediately preceding these increases shows a transient, spike-like inward current. A similar current spike

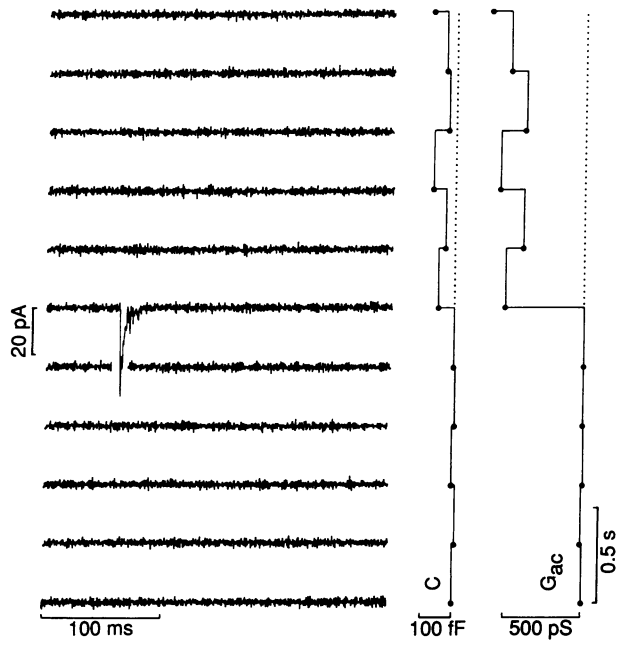

FIG. 4. (*Left*) Current collected from the fibroblast during 11 281-ms-long episodes, 1 of which shows a transient inward current. At the end of each episode, a 32-ms-long burst of sinusoidal voltage was applied to the fibroblast plasma membrane to obtain a measurement of *C* and G_{ac}. (*Right*) *C* and G_{ac} are plotted as dots connected by vertical lines; time increases upward, and *C* and G_{ac} increase leftward. The current transient is related to fusion because it tends to occur only in episodes immediately preceding the first upward jumps in capacitance or G_{ac}. This was tested in 49 fusions occurring while fibroblasts were held at negative plasma membrane potentials. We screened for transients the 10 current traces preceding the first change in capacitance or G_{ac} and the 5 current traces afterward. Transients were accepted only if their amplitude was >6 times σ_{rms}, where σ_{rms} is the root-mean-square current noise averaged over the current traces screened. By this criterion, 36 fusions showed transients in one or more of these episodes. In 30 there was only one transient, and it occurred in the episode immediately before the first capacitance or G_{ac} change. In 3 others, transients were seen also in other episodes, and, in an additional 3, a single transient was seen in an episode other than that before the first capacitance or G_{ac} change. By Poisson statistics, the chance of accidentally observing such close temporal correlation between transients and capacitance or G_{ac} changes is only 4×10^{-24}. Not all fusions were preceded by current spikes. An ≈10% failure rate is expected because transients are missed if they occur during the 10% of the duty cycle where we measure capacitance and G_{ac} but not current. The observed failure rate was actually higher because some current transients, although clearly visible, were too small to satisfy our criterion, while others were probably lost in the background noise.

shows up in none of the other traces; hence, it must be related to an early event in fusion (see Fig. 4 legend).

By analogy with similar findings on exocytic fusions in secreting mast cells (8), we suggest that the current transients represent the discharge of the RBC membrane potential through the nascent fusion pore. An alternative is that the transient current instead flows through a leak developing in the plasma membrane of the fibroblast, perhaps due to a transient and local disruption of the lipid bilayer at the fusion site. However, the following results show that such a "leak" would have to be ion selective. Current spikes were recorded in impermeant buffer (see *Methods*) from fibroblasts held at potentials varying from −78 to +14 mV. They were inward throughout, with amplitudes of −20 ± 2 pA (n = 28) at potentials around −48 mV and −10 ± 4 pA at potentials around +7 mV (n = 11). When peak current was plotted against fibroblast membrane potential (data not shown), the best-fitting straight line intersected the abscissa at +64 mV.

Although the points scatter and do not determine the intercept accurately, the reversal potential is clearly positive. If one considers those ions in our buffers that are the smallest, most mobile, and hence the most likely candidates for mediating the current spikes, then it is difficult to see how an aqueous defect in the lipid bilayer would generate a positive reversal potential. For a cation-selective defect, the most abundant small cation present in our system (internal Cs^+) would generate a negative reversal potential. For a defect that is anion selective—e.g., through protonation of phospholipid headgroups by the acidic pH—the reversal potential should be near zero because $[Cl^-]$ was the same inside the fibroblast and out. Our results are more easily explained if the current spikes flow through a fibroblast–RBC junction to equalize the membrane potentials of the two cells. Under this hypothesis, the reversal potential of the spikes would equal the membrane potential of the RBC. Because of the selective permeability of the RBC membrane to Cl^-, the RBC potential is likely to be positive at low pH and low external $[Cl^-]$ (14, 15).

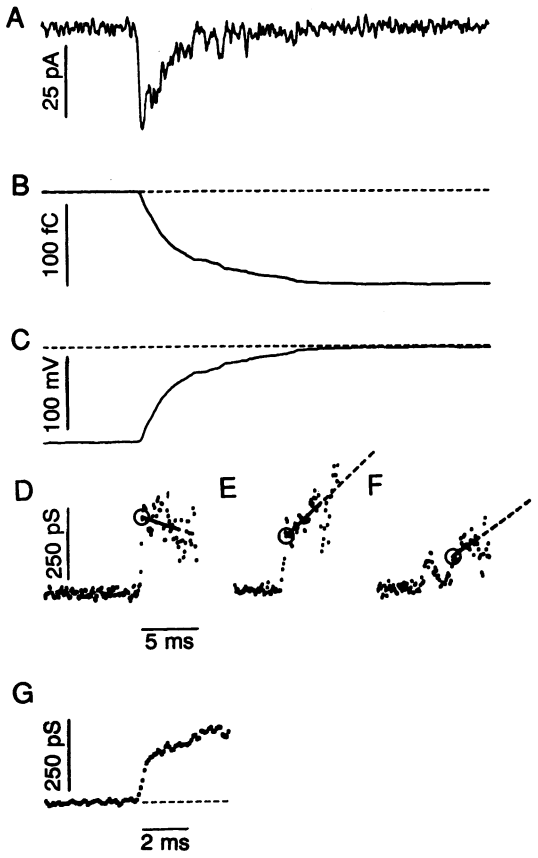

FIG. 5. (*A*) Current transient of Fig. 4. (*B*) Its time integral. (*C*) Potential across the fusion pore, obtained by subtracting trace in *B* from its final value and dividing the result by the RBC capacitance. The potential is plotted as the cytosol of the fibroblast minus that of the RBC. In this cell pair, the RBC potential (V_{RBC}) was 78 mV inside positive, 126 mV more positive than that of the fibroblast; averages were 33 ± 9 mV (n = 28) in impermeant buffer and 13 ± 8 mV (n = 10) in NaCl buffer. (*D*) Pore conductance calculated by dividing trace in *A* by trace in *C*. (*E* and *F*) Conductance traces from two other fusions. The regression lines drawn into traces in *D–F* (extrapolated for better visibility in *E* and *F*) define the initial conductances, g_i (circles). Ref. 7 describes the method of fit, the criteria for choosing the interval over which the fit is made, and for deciding which traces are suitable for analysis. (*G*) Twenty-two traces as in *D–F* were averaged after aligning them to coincide at the point where the conductance first reached a value of at least $g_i/2$ (7). To explore how abruptly fusion pores open on average, we measured the rise time, defined by the time taken for the conductance to increase from 20% to 80% of g_i. Its median value was 234 μs (n = 39; range, 68–1328 μs). To test how much of this time could be accounted for by delays in our recording equipment, we simulated an RBC and its fusion pore by a series combination of resistor and capacitor and applied exponentially blunted voltage steps to it (time constant, 73 μs). When the resulting current transients were analyzed as described above, the resulting "conductance traces" had a median rise time of 135 μs (mean, 133 ± 4 μs; range, 97–167 μs; n = 30). The voltage step was blunted because in an experiment the voltage clamp distorts the step into an exponential lag, whose time constant is the capacitance of the fibroblast times the resistance connecting the pipette interior with the cytosol (average, 73 μs; this work). Any current collected by the patch clamp will suffer a similar distortion.

The First Milliseconds of a Fusion Pore. The initial pore conductance can be obtained by analyzing current spikes (7). Fig. 5*A* shows the current spike in Fig. 4, and Fig. 5*B* shows the total electric charge moved (integral of the current). The final amplitude of the trace in Fig. 5*B* divided by the capacitance of the RBC equals the voltage between fibroblast and RBC when the pore first opens. Fig. 5*C* plots the voltage between the two cells against time; it declined to zero as the electric charge stored on the plasma membranes of the two cells redistributed. Since the trace in Fig. 5*C* represents the voltage that drove the current through the fusion pore, the pore conductance can be obtained by dividing the trace in Fig. 5*A* by that in Fig. 5*C*. As the pore opened, the conductance between the two cells increased abruptly to ≈250 pS and then changed little during the next few milliseconds (Fig. 5*D*). However, when the conductance was measured 230 ms later with a burst of sinusoidal voltage, it had increased to 550 pS and, in another 312 ms, to ≈600 pS (Fig. 1*D*). Table 1 gives average values from similar experiments. The initial pore conductances (circles in Fig. 5 *D–F*) average around 150 pS (range, 18–375 pS). By the time the first burst of sinusoidal voltage is given, the average pore conductance has grown to 400–500 pS. Both values are independent of the external buffer, consistent with the idea that fusion connects two intracellular compartments, and, at least during the first 10 s, creates no leak to the extracellular space (6).

Fig. 5 *E* and *F* shows conductance traces from 2 other fusions; Fig. 5*E* represents the response seen most often. Fig. 5*F* shows that large conductance fluctuations as in Fig. 3 can occur even on a millisecond time scale. Fig. 5*G* shows the average from 21 fusions. As in Fig. 5*E*, a conductance jump was followed by a more gradual increase. Its rate was determined by fitting a straight line to the sloping part of the trace in Fig. 5*G* (not shown), and was 37 pS/ms during the first 5 ms. At this rate, the conductance would increase from 150 to 450 pS in <10 ms.

How abruptly do fusion pores open? The median rise time of the conductance jump was 0.1 ms longer than explicable by the limited speed of our recording circuitry (see Fig. 5 legend). We conclude tentatively that g_i is not reached in a truly stepwise fashion and, hence, that the conductance jump does not represent a single conformational change in a macromolecule. This statement is based on measurements near the limit of our temporal resolution, but similar conclusions were reached also for the exocytic fusion pore (7).

Table 1. Early and late fusion pore conductances

Buffer	g_i, pS	g_c, pS	g_g, pS
Impermeant	151 ± 19 (24)	507 ± 80 (24)	446 ± 62 (24)
NaCl	154 ± 43 (6)	391 ± 69 (11)	357 ± 49 (11)

g_i, the initial pore conductance, was obtained as in Fig. 5 *D–F*. g_c and g_g are pore conductances calculated by the equations in Fig. 2 legend from the first measurements of capacitance and G_{ac} made after a spike, respectively; the small differences between g_c and g_g reflect experimental uncertainty. g_c and g_g are averages over a 31.3-ms period starting an average of 150 ms after a spike (range, 40–290 ms). Number of measurements is in parentheses.

The Fusion Pore Can Close Completely. Occasionally (3 of 65 fusions), capacitance and G_{ac} both returned to baseline levels for 10 s or more before increasing again (data not shown), suggesting that the fusion pore had closed completely. This was confirmed in two of the three fusions, where the second increase in capacitance and G_{ac} was preceded by a spike, and where the closed pore evidently allowed the RBC to regenerate its prefusion membrane potential. In one example, the pore closed after its conductance had grown from g_i = 44 pS to 600 pS. Evidently, early steps in fusion are reversible.

DISCUSSION

We have tracked the development of HA-mediated fibroblast–RBC junctions by monitoring their electrical conductance. In electrical admittance measurements (capacitance and G_{ac}), the junctional conductance could be monitored over times extending from 10 ms to minutes. The analysis of current transients allowed us to follow the first moments of a junction at submillisecond time resolution.

The first connection between the cells has a conductance ranging from tens to hundreds of picosiemens (average 150 pS). We suggest that it represents an aqueous connection that we call the fusion pore. The pore conductance increases rapidly in the subsequent 10–50 ms (Figs. 2 and 4*G*) but then fluctuates for seconds around 400–700 pS (Figs. 2*B* and 3 *B* and *C*). The junctional conductance ultimately grows beyond 10 nS, but this happens slowly (6) and sometimes in steps (Fig. 2*B*). Since under our experimental conditions RBC and fibroblast membranes are in intimate contact over several μm^2 (e.g., see figure 3 of ref. 4 and figure 1 of ref. 5), the later conductance steps may represent successive openings of additional fusion pores.

As in exocytic fusion in mast cells (7, 8), analysis of current transients shows that the viral fusion pore opens abruptly, although the transition between closed and open is probably not as rapid as with some ion channels (<10 μs in the nicotinic acetylcholine receptor; see ref. 10). As in exocytic fusion, the initial pore conductance (150 pS at 28°C as compared to ≈300 pS at 21°C–24°C in mast cells) is more variable than is usually observed in single ion channels. In both systems, the conductance grows rapidly after the pore has opened (30–40 pS/ms at 28°C in the present work, 210 pS/ms at 22°C in mast cells), suggesting that the pore dilates quickly, at least initially. Finally, viral as well as exocytic fusion pores occasionally close again even after their conductance has grown 10-fold or more. The differences are that in the exocytic pore, (*i*) g_i is somewhat larger, and (*ii*) the conductance rapidly grows to values of several nanosiemens and beyond, while with HA the growth of the pore is temporarily arrested at a conductance of ≈600 pS. The reasons for the slow and halting growth of the HA-mediated fusion pore are unclear and may be related more to the unusually dense cytoskeleton beneath the RBC membrane than to the viral fusion mechanism itself. Aside from these differences, however, the early events in exocytic and viral fusion are similar and suggest that the initial fusion pores in the two systems have common structural features.

The Fusion Pore Is Initially Small. Two methods may be used to estimate the initial diameter of the fusion pore from its conductance. First, we note that the initial pore conductance (150 pS at 28°C) is in the range of values measured for single gap junction channels at room temperature [70–180 pS in lacrimal glands (16, 17), 80–240 pS in cardiac muscle (18)]. Although viral fusion pores and gap junctions are unlikely to have molecular similarity, both structures form aqueous connections across two membranes and are thus likely to have similar lengths. On this basis, the average HA-mediated fusion pore has initially about the same diameter as a gap junction channel (1.6–2 nm; see ref. 19). Alternatively, the pore diameter can be calculated from equation 8-1 of Hille (20). For this calculation, we assume that the resistivity within the pore is that of our pipette solution (65 Ω·cm at 30°C; see *Methods*). If the pore is as long as a complete HA trimer (20.5 nm; see ref. 21), then 150 pS translates into a diameter of 1.6 nm. If, as a lower limit, the pore is just long enough (8 nm) to span two lipid bilayers, then 150 pS translates into a diameter of 1.0 nm.

Although estimates of diameters from conductances are inaccurate, the agreement between the two types of estimate points to a range of only 1–2 nm. Clearly, the initial pore has molecular dimensions. A circle of 1.3 nm diameter would result if eight phosphatidylcholine headgroups (0.8 nm diameter) in a lipid-lined pore were arranged in a ring (3). Alternatively, eight membrane-spanning α-helices spaced 1.0 nm center to center (22) would form a 1.6-nm-diameter pore in their midst if they were arranged like the staves in a barrel. Although the structure of the initial fusion pore remains unknown, the pore's small initial conductance suggests to us that it requires the participation of only a small number of HA trimers.

We thank Drs. Jonathon Howard and Frederick Tse for helpful comments on the manuscript, and Drs. Ari Helenius and Judith White for the cell line NIH 3T3HA-b2. This work was supported by National Institutes of Health Grant GM-39520.

1. Wiley, D. C. & Skehel, J. J. (1987) *Annu. Rev. Biochem.* **56,** 365–394.
2. Stegmann, T., Doms, R. W. & Helenius, A. (1989) *Annu. Rev. Biophys. Biophys. Chem.* **18,** 187–211.
3. White, J. M. (1990) *Annu. Rev. Physiol.* **52,** 675–697.
4. Doxsey, S. J., Sambrook, J., Helenius, A. & White, J. M. (1985) *J. Cell Biol.* **101,** 19–27.
5. Sarkar, D. P., Morris, S. J., Eidelman, O., Zimmerberg, J. & Blumenthal, R. (1989) *J. Cell Biol.* **109,** 113–122.
6. Spruce, A. E., Iwata, A., White, J. M. & Almers, W. (1989) *Nature (London)* **342,** 555–558.
7. Spruce, A. E., Breckenridge, L. J., Lee, A. K. & Almers, W. (1990) *Neuron* **4,** 643–654.
8. Breckenridge, L. J. & Almers, W. (1987) *Nature (London)* **328,** 814–817.
9. Ellens, H., Bentz, J., Mason, D., Zhang, F. & White, J. (1990) *Biochemistry* **29,** 9697–9707.
10. Hamill, O. P., Marty, A., Neher, B., Sakmann, B. & Sigworth, F. J. (1981) *Pflügers Arch.* **391,** 85–100.
11. Neher, E. & Marty, A. (1982) *Proc. Natl. Acad. Sci. USA* **79,** 6712–6716.
12. Colquhoun, D. & Sakmann, B. (1985) *J. Physiol. (London)* **369,** 501–557.
13. Robinson, R. A. & Stokes, R. H. (1959) *Electrolyte Solutions* (Butterworth, London).
14. Lassen, U. V. (1972) in *Oxygen Affinity of Hemoglobin and Red Cell Acid Base Status*, eds. Rørth, M. & Astrup, P. (Munksgaard, Copenhagen), pp. 290–304.
15. Lassen, U. V., Pape, L. & Vestergaard-Bogind, B. (1978) *J. Membr. Biol.* **39,** 27–48.
16. Neyton, J. & Trautman, A. (1985) *Nature (London)* **317,** 331–335.
17. Neyton, J. & Trautman, A. (1986) *J. Exp. Biol.* **124,** 93–114.
18. Veenstra, R. D. & DeHaan, R. L. (1988) *Am. J. Physiol.* **254,** H170–H180.
19. Schwarzmann, G., Wiegandt, H., Rose, B., Zimmerman, A., Ben-Haim, D. & Loewenstein, W. R. (1981) *Science* **213,** 551–553.
20. Hille, B. (1984) *Ionic Channels in Excitable Membranes* (Sinauer, Sunderland, MA), pp. 186–188.
21. Ruigrok, R. W. H., Wrigley, N. G., Calder, L. J., Cusack, S., Wharton, S. A., Brown, E. B. & Skehel, J. J. (1986) *EMBO J.* **5,** 41–49.
22. Henderson, R. & Unwin, P. N. T. (1975) *Nature (London)* **257,** 28–32.